Supporting information

Graphene Microsheets from Natural Microcrystalline Graphite Minerals：Scalable Synthesis and Unusual Energy Storage

Junying Wang,[a] Jianlin Huang,[a] Rui Yan,[a,b] Faxing Wang,[a] Wengang Cheng,[a] Quangui Guo,[a] Junzhong Wang*[a]

[a] *Key Laboratory of Carbon Materials, Institute of Coal Chemistry, Chinese Academy of Science,Taiyuan,030001, P R China.*

[b] *University of Chinese Academy of Sciences, Beijing 100049, P R China.*

**Corresponding authors. Tel: 86-351-4040407. E-mail: wangjz@sxicc.ac.cn (J. Z. Wang).*

Characterization methods

Scanning electron microscopy (SEM) images were obtained on a JSM-7001F FESEM (Field emission scanning electron microscopy). Transmission electron microscopy (TEM) images were obtained with a JEM-2100F microscope at an acceleration voltage of 200 kV. The TEM samples were prepared by dispersing in isopropanol and sonicating in a laboratory bath sonication for 5 min, and then 10 ~ 15 drops of the supernatant was dropped onto an ultrathin carbon film supported Cu TEM grids. X-ray powder diffraction (XRD) was recorded at a scan rate of 0.02 °/s using the Cu Kα (λ = 1.540600 Å) line. Raman data were measured in a Jobin-Yvon HR-800 Raman system with the 488 nm line of an Ar laser as excitation source. Thermal analysis (TG/DTA) was carried out using a thermal analyzer (Netzsch STA409PC) at a heating rate of 10 °C/min from 20 to 1000 °C in Ar. The elemental analysis was performed on an Elemental Vario BL instrument and Inductive Coupled Plasma Atomic Emission Spectrometer (ICP-AES) Thermo iCAP 6300. Electrochemical characterization was performed in Autolab instrument of PGSTAT204 and CHI 660E.

1. Extended characterizations

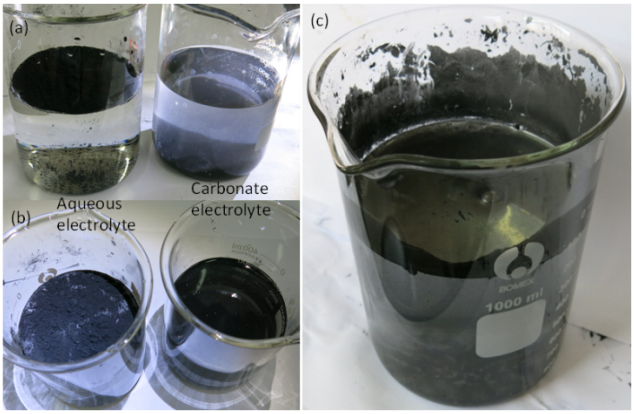

Fig. S1 Photographs show that hydrophobic/hydrophilic affinity is applied to graphene synthesis using microcrystalline graphite mineral as a precursor. (a,b) Graphite mineral powder in propylene carbonate electrolyte (right) compared with aqueous solution (0.1 M $(NH_4)_2SO_4$) electrolyte (left) in glass bakes, (a) side view, (b) top view. The two photographs present that the graphite mineral powder is aggregated and floating onto aqueous solution but precipitate down to bottom in the propylene carbonate electrolyte. (c) Mediated graphene product that was electrochemically charged and solvated in organic carbonate electrolyte is floating on the water surface due to the surface strain and hydrophobicity of graphene and organic electrolyte.

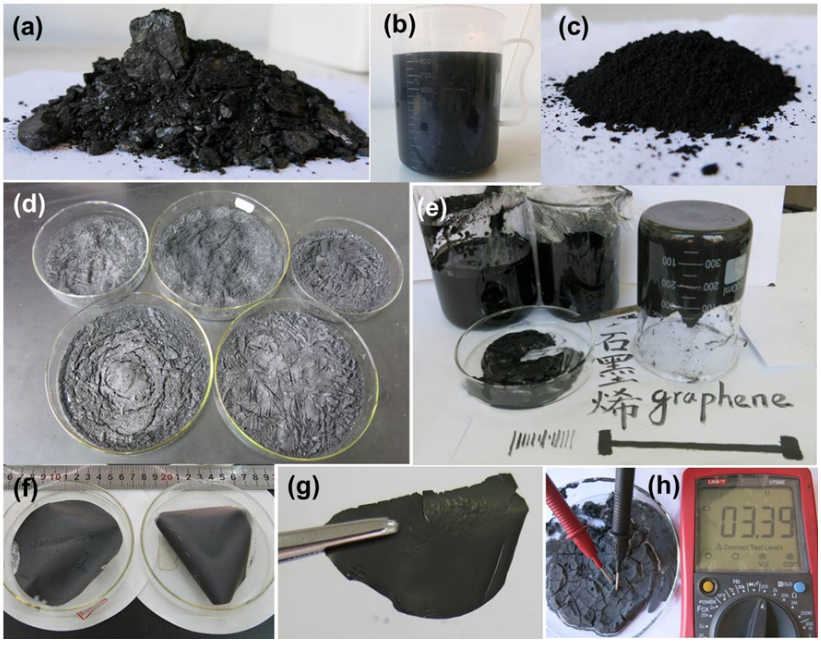

Fig. S2 Photographs of some graphene microsheets products. (a) Natural microcrystalline graphene minerals from Neimeng province in China, (b) Graphene water dispersion, (c) Graphene powder dried at 80 °C, (d) Graphene powder obtained by freeze-drying, (e) Colloidal graphene inks, (f) Graphene films filtered, (g) Free-standing graphene film, (g) Graphene powder dried in air measured by multi-meter: the electrical resistance is 3.39 ohm.

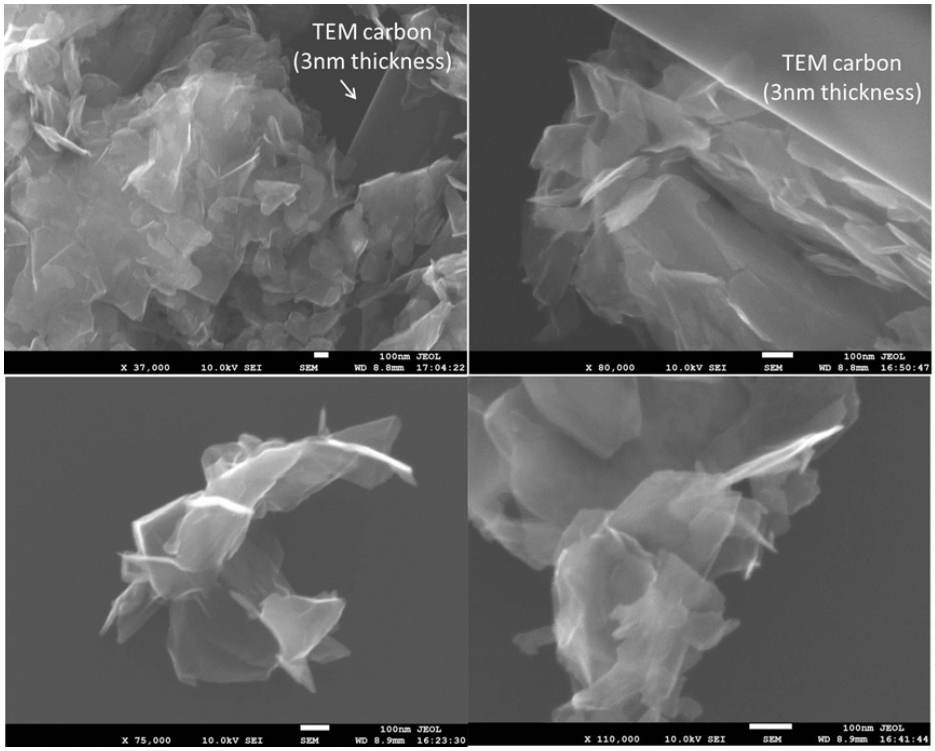

Fig. S3 SEM images of graphene microsheets that were dropped onto TEM grids with a ultrathin carbon support of 3 nm thickness. The graphene microsheets are thinner than the amorphous carbon support of TEM grids.

EDX analysis for microcrystalline graphite minerals (Fig. S4 - Fig. S5)

Two typical places of A and B for graphite minerals (Fig. S2-Fig. S3) and graphene product (Fig. S4-Fig. S5) were finely scanned.

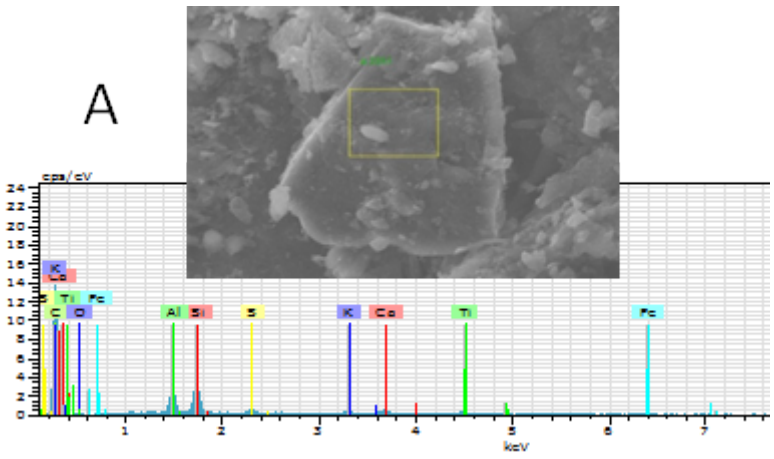

EDX analysis for microcrystalline graphite mineral

El	AN	Series	unn. C [wt.%]	norm. C [wt.%]	Atom. C [at.%]	Error (1 Sigma) [wt.%]	K fact.	Z corr.	A corr.	F corr.
C	6	K-series	45.38	**78.69**	**89.69**	5.27	1.000	1.000	1.000	1.000
Si	14	K-series	3.70	**6.42**	**3.13**	0.18	1.000	1.000	1.000	1.000
Al	13	K-series	2.57	**4.46**	**2.27**	0.15	1.000	1.000	1.000	1.000
O	8	K-series	1.64	**2.84**	**2.43**	0.37	1.000	1.000	1.000	1.000
Ti	22	K-series	1.23	2.13	0.61	0.07	1.000	1.000	1.000	1.000
Ca	20	K-series	1.17	2.03	0.69	0.07	1.000	1.000	1.000	1.000
S	16	K-series	0.71	1.23	0.53	0.05	1.000	1.000	1.000	1.000
K	19	K-series	0.64	1.10	0.39	0.05	1.000	1.000	1.000	1.000
Fe	26	K-series	0.63	1.10	0.27	0.06	1.000	1.000	1.000	1.000
		Total:	57.67	100.00	100.00					

Fig. S4 EDX scan analysis for microcrystalline graphite minerals of A place of graphite

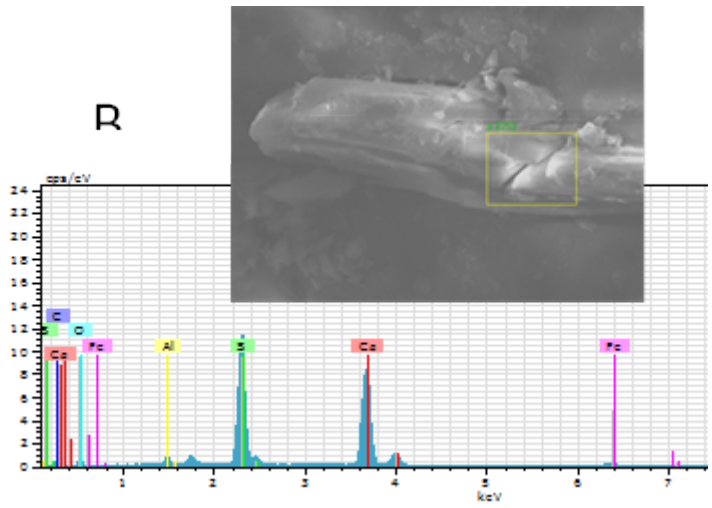

El	AN	Series	unn. C [wt.%]	norm. C [wt.%]	Atom. C [at.%]	Error (1 Sigma) [wt.%]	K fact.	Z corr.	A corr.	F corr.
Ca	20	K-series	29.94	**40.62**	**25.34**	0.92	1.000	1.000	1.000	1.000
S	16	K-series	20.04	**27.19**	**21.20**	0.73	1.000	1.000	1.000	1.000
C	6	K-series	12.71	**17.25**	**35.90**	1.92	1.000	1.000	1.000	1.000
O	8	K-series	6.65	**9.02**	**14.10**	1.10	1.000	1.000	1.000	1.000
Fe	26	K-series	3.12	4.24	1.90	0.13	1.000	1.000	1.000	1.000
Al	13	K-series	1.24	1.68	1.56	0.09	1.000	1.000	1.000	1.000
		Total:	73.70	100.00	100.00					

Fig. S5 EDX scan analysis for microcrystalline graphite minerals of B place of impurity with charging problem for SEM imaging.

EDX analysis for graphene product (Fig. S6, S7).

Two typical places of (A) and (B) were scanned.

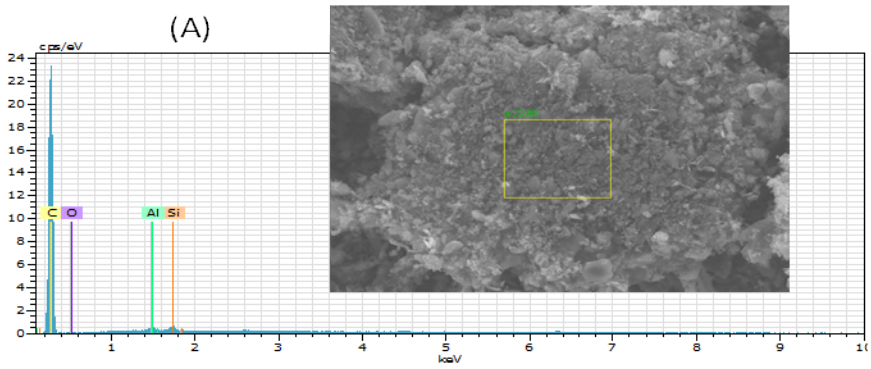

a 2249 日期: 5/8/2014 5:27:45 PM高压: 15.0kV 脉冲: 2.21kcps

El	AN	Series	unn. C [wt.%]	norm. C [wt.%]	Atom. C [at.%]	Error (1 Sigma) [wt.%]	K fact.	Z corr.	A corr.	F corr
C	6	K-series	97.59	97.59	98.72	10.99	1.000	1.000	1.000	1.000
Si	14	K-series	0.93	0.93	0.40	0.07	1.000	1.000	1.000	1.000
Al	13	K-series	0.78	0.78	0.35	0.07	1.000	1.000	1.000	1.000
O	8	K-series	0.70	0.70	0.53	0.29	1.000	1.000	1.000	1.000

Fig. S6 EDX scan analysis for graphene microsheets of A place

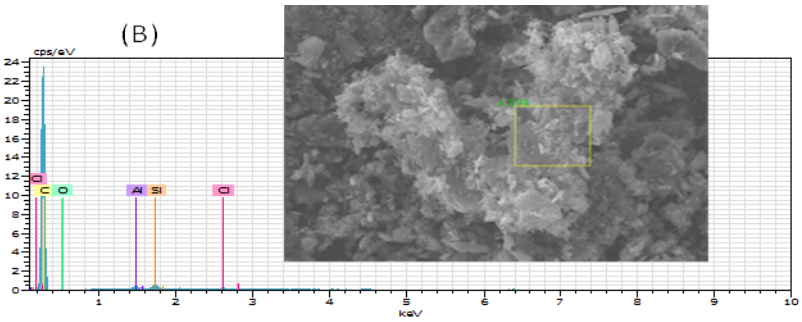

a 2248 日期: 5/8/2014 5:24:52 PM高压: 15.0kV 脉冲: 2.15kcps

El	AN	Series	unn. C [wt.%]	norm. C [wt.%]	Atom. C [at.%]	Error (1 Sigma) [wt.%]	K fact.	Z corr.	A corr.	F corr
C	6	K-series	97.58	97.58	98.73	11.06	1.000	1.000	1.000	1.000
Si	14	K-series	0.87	0.87	0.38	0.07	1.000	1.000	1.000	1.000
O	8	K-series	0.72	0.72	0.54	0.31	1.000	1.000	1.000	1.000
Al	13	K-series	0.62	0.62	0.28	0.06	1.000	1.000	1.000	1.000
Cl	17	K-series	0.22	0.22	0.07	0.04	1.000	1.000	1.000	1.000

Fig. S7 EDX scan analysis for graphene microsheets of B place

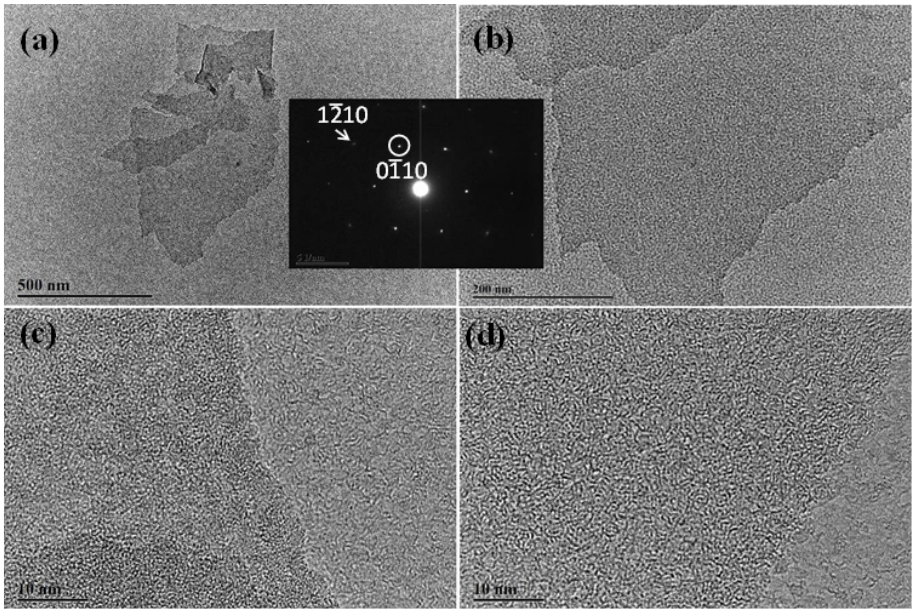

Fig. S8 TEM images of single layer graphene microsheets. (a,b) Low magnification, (c,d) High resolution. Inset SAED pattern: the intensity ratio of $\{0\bar{1}10\}$ plane is stronger than $\{1\bar{2}10\}$ plane.

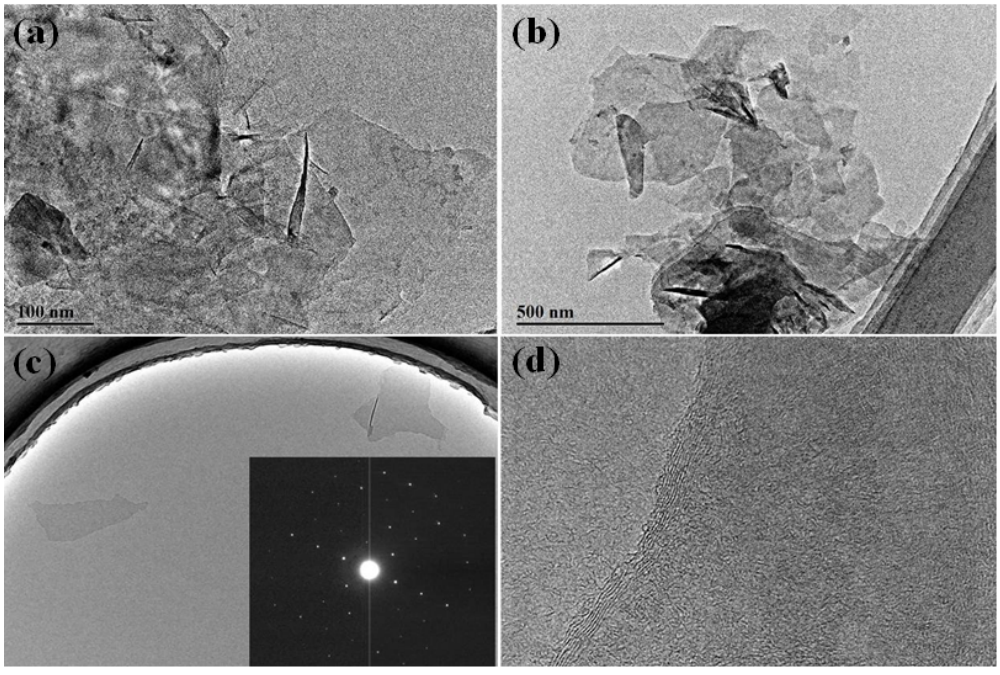

Fig. S9 TEM images of few-layer graphene microsheets. (a,b) Low magnification TEM images of graphene microsheets, (c) Two pieces of graphene microsheets, inset ED pattern. (d) High resolution TEM image showing 6 layers.

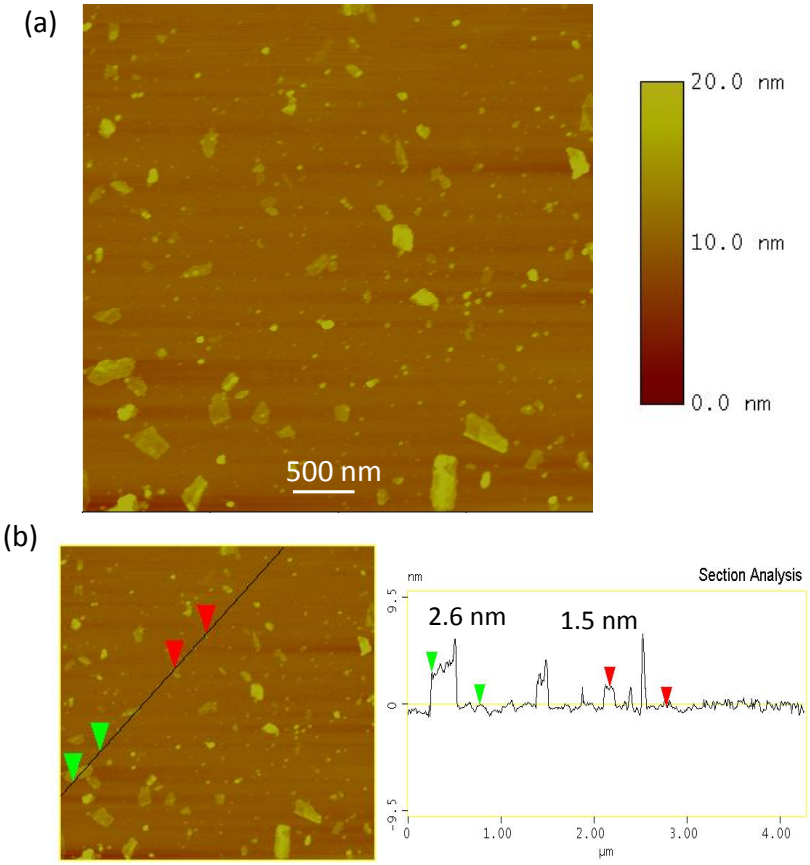

Fig. S10 AFM data of graphene microsheets on a Si substrate. (a) A number of isolated graphene microsheet and stacked graphene microsheets were shown in the AFM image. (b) Section analysis shows the thickness of the graphene marked is 1.5 nm and 2.6 nm, which may indicate of 2-4 atomic layers of graphene.

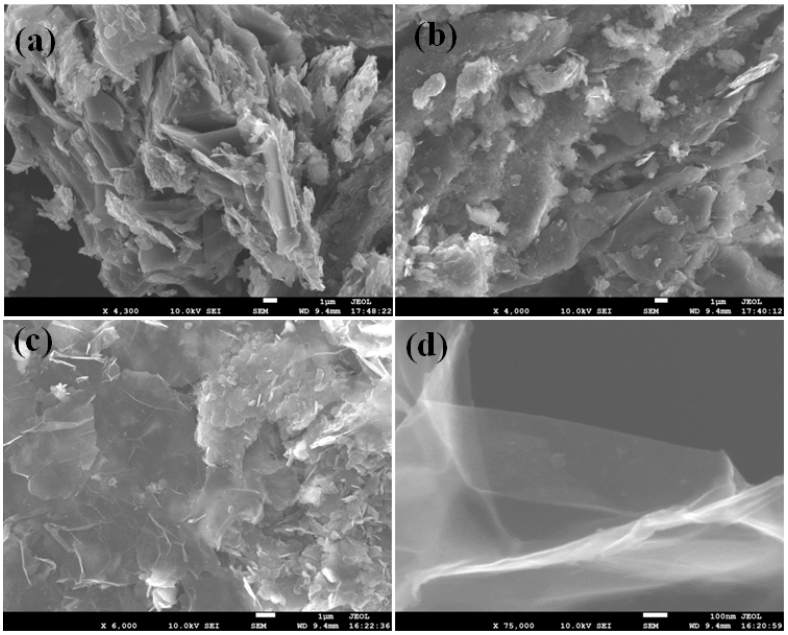

Fig. S11 SEM images of (a,b) graphite minerals from Neimeng province and (c,d) its product of graphene microsheets. This mineral has ~10 wt% of flake graphite and ~70 wt% microcrystalline graphite. Thus the graphene products has correspondingly graphene flakes of > 10 μm sheet size and graphene microsheets of < 1 μm sheet size. This data indicate that this graphene synthesis process can be generally applied to different type of graphene minerals.

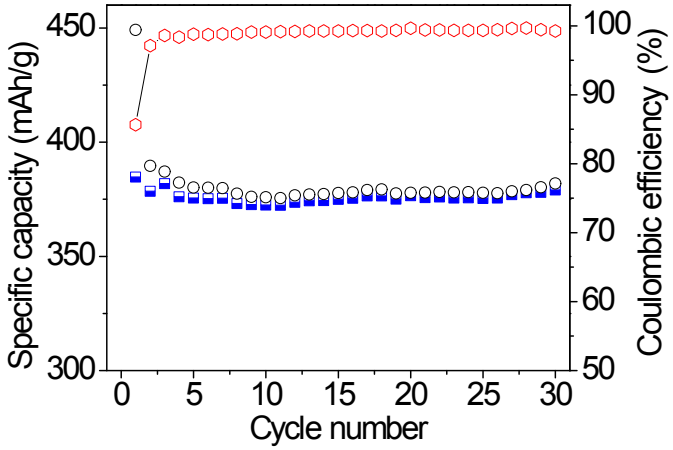

Fig. S12 Specific capacity and coulombic efficiency versus cycle index. The graphene microsheets are used as the anode of Li ion battery without annealing (lithium metal foil as cathode).

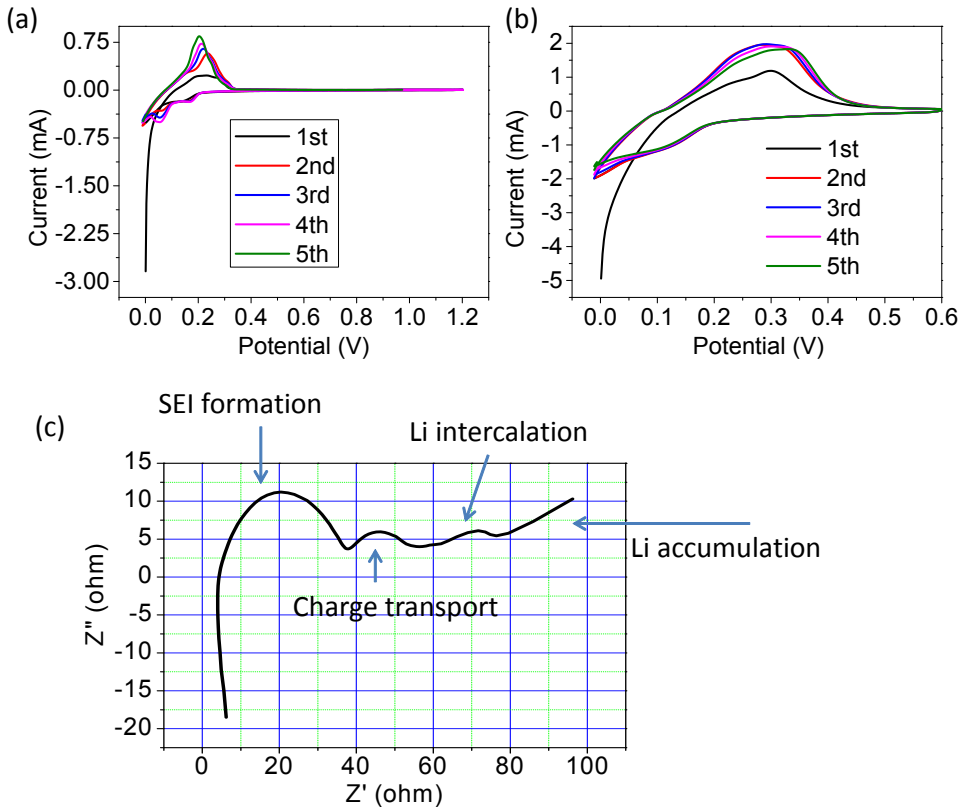

Fig. S13 (a) Cyclic voltammograms (CV) curve in the potential range of 0 - 1.2 V with slow scan rate of 0.1 mV/s (The 0 - 0.5 V CV is presented as Fig. 4b). The current increases with cycles. The peak at 0.2 V is assigned to Li lithiation of graphene microsheets (GM) and the peaks at 0.05 V and 0.17 V probably result from deintercalation of Li from GM. (b) CV curve in the potential of 0 - 0.6 V with the scan rate of 1.0 mV/s. The current decreases with cycles. (c) AC impedance spectrum of graphene anode lithium ion battery in a frequency range from 100 kHz to 1 Hz. The label shows the possible origins for impedance at 4 frequency regions.

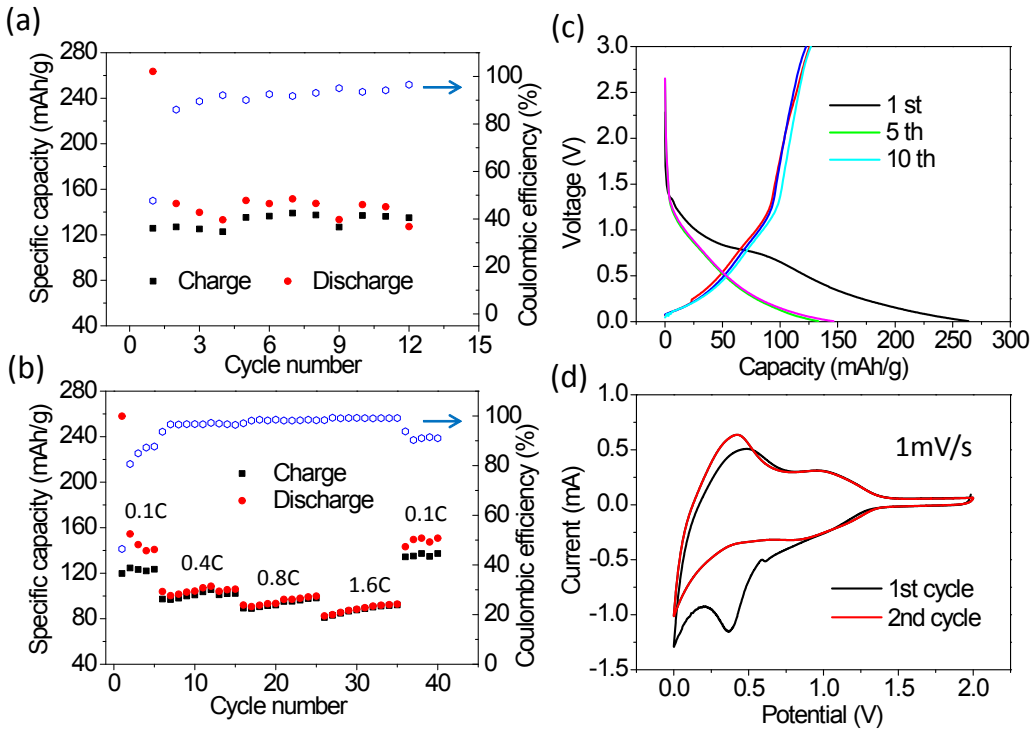

Fig. S14 Electrochemical performances of commercial carbon black (Super P) anode for lithium ion batteries (The carbon black loading for the electrodes is around 1.1 mg/cm^2. Lithium metal foil worked as cathode). (a) Specific capacity and coulombic efficiency (CE) versus cycle index (first specific capacity is 263.6 mAh/g, and first CE is 47.6%, and average CE of 11 cycles after first cycle is 90.1%.) The voltage range of charge/discharge is 0.001 V - 3.0 V. (b) Rate capacity and coulombic efficiency versus cycle index. The discharge/charge current density ranges from 37 mA/g (0.1 C) to 595 mA/g (1.6 C) (average CE of 39 cycles after first cycle is 95.7%). (c) Voltage profiles of the anodic half-cell have no lithiation–delithiation plateau. (d) The cyclic voltammograms (CV) curves of 1st and 2nd cycles at slow scan rates of 1 mV/s.